JOURNAL OF CATALYSIS 67, 430–445 (1981)

Hydrodesulfurization Catalysis by Transition Metal Sulfides

T. A. PECORARO AND R. R. CHIANELLI[1]

Corporate Research Laboratories, Exxon Research and Engineering Company, Linden, New Jersey 07036

Received May 11, 1980; revised September 15, 1980

The primary effect in the hydrodesulfurization of dibenzothiophene by transition metal sulfides is "electronic," i.e., it is related to the position the metal occupies in the periodic table. This effect, which determines the ability of the transition metal sulfides to catalyze the HDS reaction, varies over three orders of magnitude across the periodic table. The first-row transition metal sulfides are relatively inactive, but the second- and third-row transition metals show maximum activity with Ru and Os. HDS activity as a function of periodic position yields typical "volcano" plots.

INTRODUCTION

Hydroprocessing catalysts based upon the transition metal sulfides have been widely used for over 60 years and catalysts such as $Co/Mo/Al_2O_3$ remain the industry "workhorses" in hydroprocessing of petroleum-based feedstocks (*1*). Applications have included sulfur removal (hydrodesulfurization), nitrogen removal (hydrodenitrogenation), and product quality improvement (hydrotreating, hydroconversion). Original interest (prior to WW II) in these catalysts centered on their activity in the hydrogenation of coal liquids which contain considerable amounts of sulfur maintaining the transition metal in the sulfided state. Co, Ni, Mo, W sulfides and their mixtures were recognized as the most active and least expensive of the transition metal sulfides (*2*). Later (post-WW II) their major uses shifted to hydroprocessing of sulfur- and nitrogen-containing petroleum-based feedstocks with Co- and Ni-promoted Mo and W catalysts usually supported on Al_2O_3. Today, however, as petroleum feedstock supplies dwindle, the processing of "dirtier" feeds containing larger amounts of sulfur, nitrogen, and metals increases. In order to achieve this in the future, a new generation of transition metal sulfide-based catalysts are needed which have higher activities, greater selectivity to desired products, and greater resistance to poisons. In spite of the past and future importance of sulfide catalysts, little is understood regarding the general fundamental basis for an origin of their catalytic activity. A starting point for this understanding lies in the knowledge of the solid-state properties of the transition metal sulfides, in particular the relation between bulk properties and surface behavior. Perhaps the most explicit solid-state picture of the sulfided form of these catalysts is the "pseudo-intercalation" model proposed by Voorhoeve and Stuiver (*3*) for Ni-promoted WS_2 catalysts. In this picture anion vacancies at the edge of WS_2 crystals are electronically promoted via charge transfer from intercalated Ni atoms of the W atoms in the bulk WS_2. Yet progress in confirming this model has been hampered by lack of understanding of the binary transition metal sulfides themselves, especially in catalytic environments.

The binary sulfides are quite complex in their own right. A recent publication describes the low-temperature precipitation of an amorphous MoS_2 (*4*). When annealed in H_2S/H_2 at 400°C, this amorphous phase converts into an unusual poorly crystalline form, termed the "rag" structure, consisting of several stacked but highly folded and

[1] Author to whom correspondence should be addressed.

0021-9517/81/020430-16$02.00/0
Copyright © 1981 by Academic Press, Inc.
All rights of reproduction in any form reserved.

disordered S–Mo–S layers (*5*). The determination of this structure demonstrates the flexible and macromolecular nature of layered transition metal dichalcogenides and provides a basis for understanding the relationship between its highly broadened X-ray diffraction pattern and relatively low BET surface area. Thus the method of preparation and pretreatment significantly effects the morphology of the layered dichalcogenides. This work has been extended (*6*) to correlate the HDS activity of MoS_2 catalysts (prepared by varied methods) and their edge–plane specific O_2 chemisorption capacity. The O_2 chemisorption distinguishes among catalysts of different preparations and reflects the wide variations in the edge/basal plane ratio among the various preparations.

In this paper, the results of a systematic study of the hydrodesulfurization (HDS) activity (for dibenzothiophene) of simple binary sulfides are discussed. The HDS activity is correlated with the position of the metal sulfide occupied in the periodic table and the heat of formation of the bulk sulfides. The objective of this work is to establish a link between the solid-state chemistry and physics of uniformly prepared bulk sulfides and their HDS activity.

EXPERIMENTAL

Hydrodesulfurization Activity Evaluation

1. Materials

All the chemicals were used without further purification. The dibenzothiophene, biphenyl, Tetralin, and quinoline were purchased from Aldrich Chemical Co. The Decalin was obtained from MCB. The 15% H_2S/H_2 mixture was purchased from Scientific Gas Company.

2. Feed

The standard organosulfur feed was prepared by dissolving 4.4 g of dibenzothiophene (DBT) in 100 cm^3 of hot Decalin. This solution contained about 5 wt% DBT or 0.8 wt% S. The hot solution was filtered and 1 cm^3 of decane was added.

3. Operation Procedure

The hydrodesulfurization evaluations were done in a Carberry-type autoclave. The reactor was designed to allow a constant flow of hydrogen through the feed during the activity evaluation and also to permit liquid sampling during operation.

The catalyst (1 g) was pressed under 15,000–20,000 psi and then meshed through 10/20 mesh (2.0/0.841 mm) or 20/40 mesh (0.841/0.420 mm) sieves. In a typical HDS run, the catalyst basket was charged with a mixture of 1 g of the catalyst and 10 g of 1/16-in. spheroid porcelain beads. The remainder of the basket was filled with more beads. The reactor system was then flushed with helium for about 30 min. After the helium flush, the switch was made to 15% H_2S/H_2. The catalyst was presulfided for 90 min at 25–400°C with a flow rate of 50–60 cm/min. The catalyst system was stirred during the pretreatment. The reactor was cooled (400–25°C) under flowing H_2S/H_2. When cool, the H_2S/H_2 flow was terminated and the H_2 flow started at a rate of 100 cm^3/min. At this point the reactor was charged with 100 cm^3 of the DBT/Decalin feed. The reactor was then set to the desired pressure and temperature and a gc sample was taken. Another gc sample was taken when the reactor reached the desired temperature and again at 1-hr intervals thereafter.

4. Gas Chromatography

The products were analyzed with a Perkin–Elmer 900 gas chromatograph. The operating conditions were: detector, flame ionization; columns, 10 ft, 1/8 in. 10% SP2100, 80/100 Supelcoport, D2668 Supelco; injection rod, 350°C; manifold, 250PC; program temperatures, 100–300°C; heating rate, 16–24°C/min.

Catalyst Preparation

Of prime concern in this study is the

uniform preparation of the transition metal sulfides across the periodic table. The technique which was developed to achieve this has been previously described for the Group IV–VII transition metal sulfides (*4*) and for Group VIII (*7*). This technique involves the precipitation from nonaqueous solution of the amorphous transition metal sulfide starting with the corresponding transition metal halide and a sulfide source. This procedure yields materials of moderate surface area (~10–60 m^2/g). Prior to activity testing, the catalysts are pretreated in H_2S for 1 hr at 400°C, washed with 12% acetic acid to remove LiCl produced in the reaction, then treated again at 400°C in 15% H_2S/H_2. This procedure converts the amorphous sulfides to the poorly crystalline sulfide phase shown in Table 1 (as determined from X-ray diffraction).

Examples of preparations for some of the most active catalysts are included. All other preparations are done in an analogous fashion and the reader is referred to Refs. (*4, 5, 7*) for further details.

TABLE 1

Stable Binary Sulfides

H_2S (400°C)[a]	H_2/15% H_2S (400°C)[a]	HDS reactor[b]
Cr_2S_3	Cr_2S_3	Cr_2S_3
MoS_2	MoS_2	MoS_2
WS_2	WS_2	WS_2
MnS	MnS	MnS
ReS_2	ReS_2	ReS_2
FeS_2	FeS_x	FeS_x
RuS_2	RuS_2	RuS_{2-x}
OsS_2	—	$Os^0 + S$
CoS_2	Co_9S_8	Co_9S_8
Rh_2S_3	Rh_2S_3	Rh_2S_3
IrS_3	—	$Ir^0 + S$
NiS_2	NiS_x	Ni_3S_2
PdS	PdS	PdS
PtS	PtS	PtS

[a] Predicted stable phase by thermodynamic calculations (*8*) and confirmed by X-ray diffraction.

[b] Stable phases were determined by X-ray diffraction; reaction condtions: $T = 400°C$, $P = 450$ psi, gas = H_2.

1. Group VII Sulfides

ReS_2. ReS_2 was prepared from either the penta- or tetrachloride. In a typical preparation, 2.0 g $ReCl_4$ were dissolved in 100 ml of the ethyl acetate and 1.12 g Li_2S were added with stirring. After 4 hr of stirring, the solution was filtered to yield a black powder, amorphous ReS_2. The solid was heat treated in a tube furnace for 2 hr in H_2S or 15% H_2S/H_2 at 400°C for 2 hr. Once precipitated and heat treated, the materials were stable enough to wash with 12% acetic acid to remove the residual LiCl. The material was then heat treated with H_2/H_2S (1–15% H_2S) at 400°C for 1 hr. X-Ray analysis showed the product to be poorly crystalline ReS_2 (yield 1.46 g, theoretical 1.55 g). A typical analysis for ReS_2 was: theoretical, Re = 74.39, S = 25.61; observed, Re = 74.40, S = 25.49. If the pentachloride, $ReCl_5$, was used a sulfur-rich product, $ReS_{2.5}$ was obtained at room temperature. However, it decomposed to the stoichiometric sulfide after heat treatment at 400°C in 15% H_2S/H_2.

2. Group VIII Sulfides

RuS_2. RuS_2 may be prepared from $RuCl_4$ or $RuCl_3$ (RIC/ROC). In a typical preparation 7.4 g of $RuCl_4$ was dissolved in 100 ml of ethyl acetate and 2.80 g Li_2S (Ventron) was added with stirring. After 4 hr of stirring, the solution was filtered yielding a black powder which was still wet with ethyl acetate. The filtrate was partially green indicating suspended particles of RuS_2. The sample was then heat treated in pure H_2S at 400°C for 1.5 hr, cooled to room temperature, washed with 12% acetic acid, filtered, and heated again in 15% H_2S/H_2 for 1.5 hr. This procedure yielded pure RuS_2 as determined by X-ray diffraction and chemical analysis. If pure H_2S were used the RuS_2 would contain excess sulfur.

OsS_2. Four grams of $OsCl_4$ was added to 100 ml of ethyl acetate yielding a greenish solution. Then 1.12 g of Li_2S was added as

the solid and the solution turned black with stirring. The solution was filtered and a black powder was obtained which was treated at 400°C in a stream of H_2/15% H_2S for 2 hr. The resulting black powder weighed 2.80 g (theoretical = 3.10 g) with a BET surface area of 20 m^2/g. X-Ray analysis indicated that the OsS_2 was a previously unknown layered compound which could be converted to the known pyrite type by heating under vacuum at 600°C (*9*).

Rh_2S_3. Rh_2S_3 was prepared from $RhCl_3$ in analogous fashion to the catalysts described above:

$$2\ RhCl_3 + 3\ Li_2S \rightarrow Rh_2S_3 + 6\ LiCl.$$

X-Ray analysis before and after reaction indicated the presence of Rh_2S_3 which had a BET surface area of 15 m^2/g.

IrS_x. $IrCl_4$ (2.00 g) was dissolved in 175 ml of ethyl acetate. To this 0.55 g of Li_2S was added neat with the color changing from a dark brown to gold. After stirring for 3.5 hr a golden powder was recovered. Then 1.8 g of the product was heat treated in 15% H_2S for 2 hr, washed in 12% acetic acid then reheated in 15% H_2S for 2 hr yielding a black powder. X-Ray diffraction yielded a very diffuse powder pattern indicating IrS_x with the pyrite structure.

PdS and PtS. Both platinum and palladium were fairly inactive in the model reaction and thus their activities were not greatly affected by the methods of preparations. Thus, for this group commercially (Ventron) available compounds were also activity tested. PdS and PtS are the stable species in the reactor. PdS was prepared from the dichloride in a manner similar to that for the compounds previously described:

$$PdCl_2 + Li_2S \rightarrow PdS + 2\ LiCl.$$

PtS was prepared in this manner but was also prepared from the tetrachloride. This reaction led to chemical results differing from previous examples:

$$PtCl_4 + 2\ Li_2S \xrightarrow[\text{acetate}]{\text{ethyl}} PtS_2 + 4\ LiCl, \quad \text{(a)}$$

$$PtS_2 \xrightarrow[H_2S]{400°C} PtS. \quad \text{(b)}$$

$PtCl_4$ (1.0 g) was dissolved in 200 ml of ethyl acetate and then divided into samples. A 100-ml sample was allowed to stand; upon standing the solution began to darken and precipitation began to occur. A golden film began to form, as well as crystals. The crystals when examined under polarized light were highly pleochroic, transmitting light perpendicular but not parallel to their long axes indicating the formation of a Pt chain complex. Preliminary chemical analysis indicates a $PtCl_4$:LiCl:ethyl acetate complex. Treatment of the remaining portion of the solution with Li_2S as in previous examples yielded PtS after heat treating.

RESULTS

Catalytic Materials

Composition. The technique used for the preparation of the transition metal sulfides (TMS) was developed as part of a program to investigate their solid-state (*4*, *5*) and catalytic properties (*6*). Since aqueous precipitation caused hydrolysis of the transition metal ion with resulting hydroxide and oxide formation, the Group IV–VII sulfides required a nonaqueous preparation. This tendency to form the hydroxide or oxide diminishes across the transition series; thus Group VIII sulfides can be precipitated from aqueous solution. The non-aqueous precipitation offers a uniform method of preparation for Group IV through Group VIII sulfides and removes the factor of oxide and hydroxide formation.

The initial composition of the amorphous sulfide is dependent on the starting halide

as shown below:

$$ReCl_5 + 2.5\ Li_2S \xrightarrow[\text{ethyl acetate}]{25°C} ReS_{2.5} + 5\ LiCl, \quad (1a)$$

$$ReS_{2.5} \xrightarrow[H_2S/H_2]{400°C} ReS_{2.0} + 0.5\ S°, \quad (1b)$$

$$ReCl_4 + 2\ Li_2S \xrightarrow[\text{ethyl acetate}]{25°C} ReS_2 + 4\ LiCl, \quad (2a)$$

$$ReS_2\ (\text{amorphous}) \xrightarrow[H_2S/H_2]{400°C} ReS_2\ (\text{poorly crystalline}). \quad (2b)$$

Particularly in the case of ReS_2, the final products display significant differences in catalytic hydrodesulfurization. The origin of this difference is undoubtedly the result of the anisotropic micromorphology of the layered structure of ReS_2 as in the case of MoS_2 (*6*). Initial results show that the effect of anisotropy is less important in a compound such as RuS_2, but further work must be done to confirm this result. Because of these effects, catalysts are prepared from the tetrachloride where possible.

Further treatment is necessary to generate the catalysts to be evaluated. Once precipitated, the materials are heat treated at 400°C in H_2S (or H_2S/H_2) and then washed with 12% acetic acid to remove residual LiCl. A second treatment with H_2S/H_2 (1–15% H_2S) at 400°C produces the final catalyst. This final heat treatment often produces the sulfide phase which is stable under catalytic conditions as shown in Table 1. The exceptions are OsS_2, IrS_3, CoS_2, FeS_2, and NiS_2. Under reaction conditions, OsS_2 and IrS_3 are reduced to the metal and CoS_2, FeS_2, and NiS_2 are converted to the metal-rich sulfides as shown in Table 1.

Physical properties. Knowledge about amorphous and poorly crystalline transition metal sulfides in the literature is extremely sparse. A preliminary study using X-ray line-broadening techniques and BET surface area measurement attempts to explain the nature of the HDS catalysts. Most information deals with Group VI and VII layered sulfides and Group VIII materials. The particle sizes are calculated using

$$D = \text{particle diameter in Å} = \frac{k\lambda}{\beta \cos \theta}, \quad (3)$$

where $k = 1.05$ for most spherical and cubic particles. For the layered materials this value may be erroneous for the in-plane vectors (*9*).
$\lambda = 1.5418$ Å,
β = linewidth at half-height in radians.

X-Ray and BET data for some of the fresh and activity-tested catalysts are summarized in Table 2. The crystalline sizes vary vastly, (14 to 324 Å), while the surface area variation is significantly less (11 to 73 m^2/g). With the exceptions of Rh_2S_3, PdS, and PtS, where the crystalline sizes (as obtained by X-ray line broadening) agree with the BET surface area, the other crystallite sizes indicate higher surface areas than actually measured by BET techniques.

Layered Sulfides

In the case of the Group IV–VI layered sulfides, the MoS_2 and ReS_2 systems are characterized in detail. The catalytic MoS_2 exists in a poorly crystalline "rag" structure (*5*). Line-broadening analyses suggest an average X-ray crystalline size of 28 Å in the *c* direction and 78 Å in the *a* direction. Crystallites of these dimensions should have surface areas of several hundred square meters per gram but the actual catalyst has a BET surface area of 50 m^2/g. Transmission electron miscoscopy indicates that the *a*-axis dimension is several thousand angstroms. Thus for these mate-

TABLE 2

Physical Properties of Fresh and HDS Activity-Evaluated Binary Sulfides

Sulfide	Structure	*hkl*	β	Particle size (Å)	BET surface area (m^2/g)
Fresh					
MoS_2	Layered	100	2.1	46	50
		110	2.2	49	
		002	2.8	34	
ReS_2	Layered	110	2.2	49	7
		002	3.3	29	
OsS_2	Layered	101	2.9	35	15
IrS_{2+x}	Pyrite	200	7.0	14	73
Activity-Evaluated					
MoS_2	Layered	100	2.2	44	17
		002	2.0	46	
WS_2	Layered	100	2.0	—	—
		002			
ReS_2	Layered	—	—	—	—
Os^0 + S	Metal	101	2.9	35	15
RuS_2	Pyrite	200	1.2	90	52
Rh_2S_3	Rh_2S_3	200	0.6	162	15
Ir^0 + S	Metal	110	1.2	82	15
PdS	PdS	200	0.3	324	—
PtS	Cooperite	110	0.5	202	11

rials, the X-ray measurements represent the average unstrained repeat distances (order length) within the rags.

ReS_2 which is prepared from $ReCl_5$ and pretreated at 400°C in H_2S/H_2 exists as spheres in the range 0.1–1.0 μm illustrated by SEM in Fig. 1. The calculated surface area of these spheres, ~10 m^2/g. agrees with the measured BET areas. A comparison between the powder diffraction patterns of crystalline ReS_2 and the nonaqueous-prepared ReS_2 (after the 400°C H_2S/H_2 pretreatment) indicates that the latter is also a "poorly crystalline" layered material; see Fig. 2. X-Ray line-broadening measurements give the local areas of order to be 74 Å (100) by 35 Å (002).

Group VIII Sulfides

For the Group IV-VII transition metals the most stable phase is the layered disulfide. However, for the Group VIII metals the stable sulfide phase is dependent on the sulfur partial pressure as shown in Table 1. A brief description of the Group VIII catalysts after the HDS reaction is included.

Ruthenium disulfide. A well-defined pyrite X-ray pattern with no shift in lattice parameters from pure $RuS_{2.0}$ is obtained for the activity-evaluated catalyst. The average particle size of the crystallites is ~100 Å (line-broadening analyses). Although the pyrite structure is stable at 400°C in pure H_2S, 15% H_2S/H_2, and under reactor conditions, the sulfur content varies. For example, in pure H_2S the RuS_2 contains excess sulfur; under reactor conditions a considerable sulfur deficiency occurs, yielding a formula of $RuS_{1.7}$.

Osmium disulfide. Osmium disulfide is isolated in a layered structure by the nonaqueous precipitation followed by a heat treatment with pure H_2S at 400°C. The X-ray spectrum appears very similar to ReS_2 (Fig. 2), but with different lattice parame-

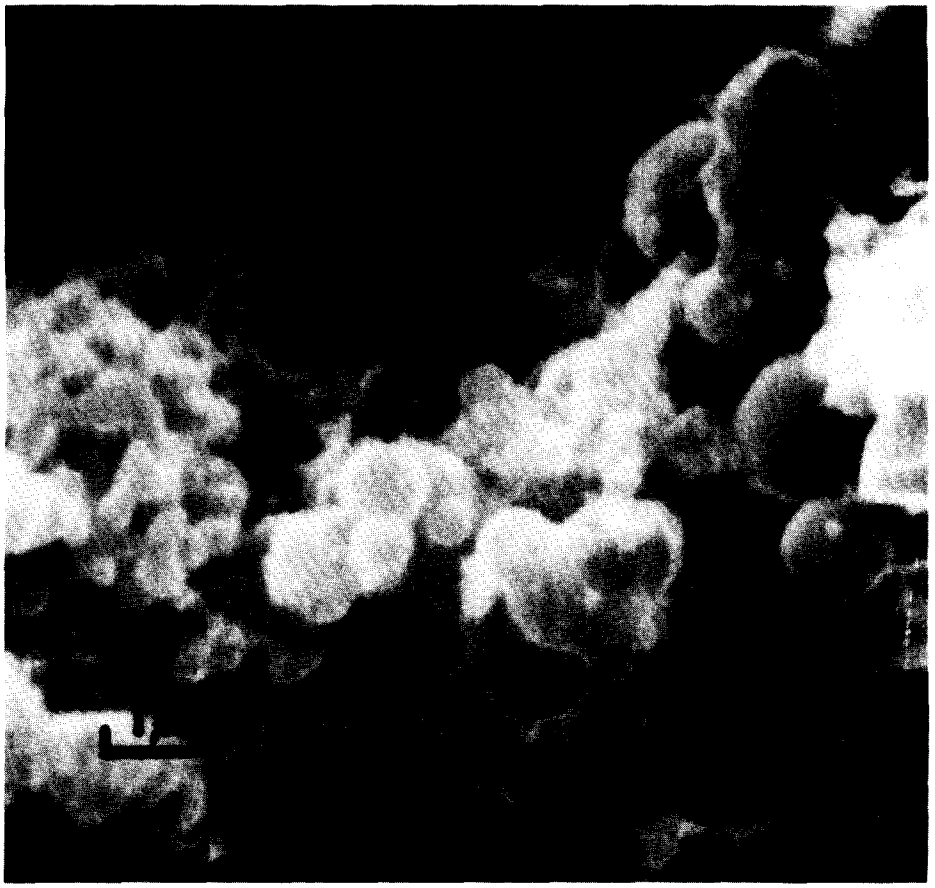

FIG. 1. ReS_2 spheres SEM.

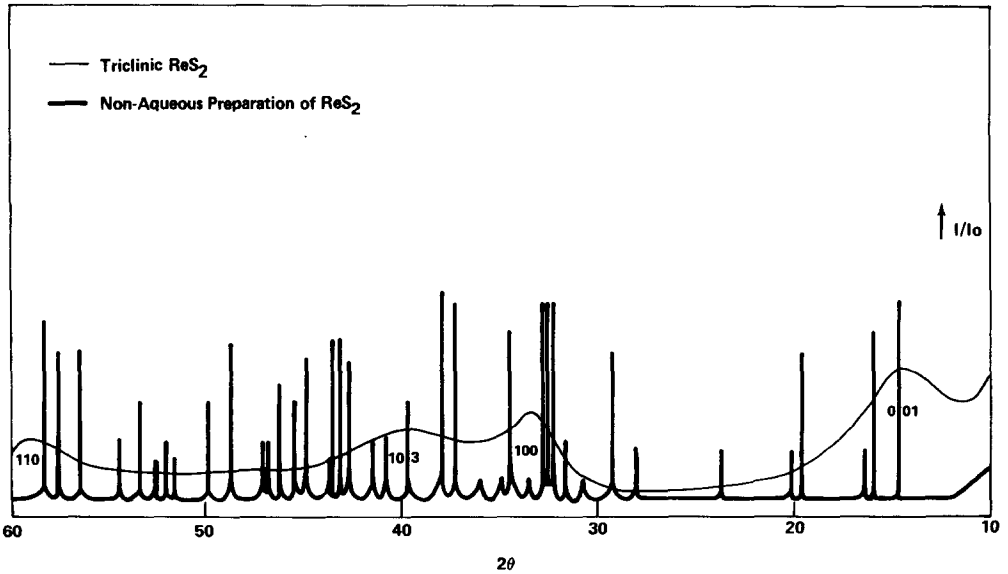

FIG. 2. X-Ray comparison of crystalline triclinic with *para*-crystalline ReS_2.

ters. Previously, OsS_2 was not known to exist in a layered structure but was reported to have a pyrite structure. In 15% H_2S/H_2 or under reactor conditions, the layered OsS_2 converts to a material which gives an osmium metal powder pattern. The X-ray lines are very broad and indicate an average crystallite size of ~35 Å. Although the existence of Os metal as the stable phase is supported by X-ray crystallography and thermodynamic calculations, the final catalyst still contains sulfur. The nature of this phase is still under investigation.

Iridium sulfide. The fresh iridium sulfide, IrS_3 (determined by chemical analysis), displays substantial amorphous character. The X-ray pattern shows that IrS_3 can have the pyrite structure with a crystallite size of 14 Å. Iridium sulfide, like the OsS_2, converts to the metal plus sulfur under reactor conditions.

Hydrodesulfurization Activity

At 400°C, the product of the HDS of DBT consists of biphenyl, except in the case of RuS_2 where some cyclohexylbenzene is formed. In order to obtain the rate constants, the disappearance of DBT, up to 50 mole% conversion (or the appearance of product(s)) is plotted against time. In this regime, linear concentration-vs-time plots are obtained; see Fig. 3. Thus, in the absence of knowledge about the true kinetics under our conditions (although preliminary data suggested that the order of the reaction is less than 1) the zero-order rate constants (slopes of the linear concentration-vs-time plots) provide a relative measure of the catalytic activity; see Table 3.

Maximum activity is obtained with the second- and third-row transition metals: in particular, the Group VIII metal sulfur systems are most active on a per gram of

TABLE 3

HDS Activity (at 400°C) and Thermodynamic Properties of the Sulfides

	Stable phase H_2/15% H_2S (400°C)	Stable phase reactor (400°C)	ΔH formation (*10*) (kcal/mole of metal)	Molecules of DBT converted M^2-sec × 10^{16} (400°C)	Molecules of DBT converted/mmole metal-sec × 10^{16} (400°C)	Molecules of DBT converted/g-sec × 10^{16} (400°C)
Ti	TiS_2	—	97.3 ± 8	0.1	1.4	0.7
V	VS_x	VS_x	—	—	1.1	1.0
Cr	Cr_2S_3	Cr_2S_3	80 ± 15	0.1	4.8	4.7
Mn	MnS	MnS	51 ± 5	0.4	0.6	0.7
Fe	FeS	FeS_x	24 ± 1	—	1.1	0.9
Co	Co_9S_8	Co_9S_8	22.6 ± 1	0.3	1.4	1.5
Ni	NiS_x	Ni_3S_2	17.2 ± 1	0.4	1.5	1.6
Zr	ZrS_2	—	138 ± 5	—	1.2	0.8
Nb	NbS_2	—	84.8 ± 4	—	1.7	1.1
Mo	MoS_2	MoS_2	65.8 ± 1	0.3	8.0	5.0
Tc	—	—	53.5 ± 5	—	—	—
Ru	RuS_2	RuS_{2-x}	49.2 ± 5	3.9	379.5	230
Rh	Rh_2S_3	Rh_2S_{3-x}	31.4	4.7	106.1	70.0
Pd	PdS	Pds	16.9 ± 1.5	1.1	12.5	9.0
Sn	SnS_2	—	—	—	1.6	0.5
Hf	HfS_2	—	—	—	—	—
Ta	TaS_2	—	84.6 ± 4	—	1.1	0.4
W	WS_2	WS_2	62 ± 4	—	3.2	1.0
Re	ReS_2	ReS_2	42.7 ± 3	1.3	39.4	20.0
Os	OsS_2	Os^0 + S	35.3 ± 3	5.7	216.3	85.0
Ir	IrS_2	Ir^0 + S	31	4.5	171.8	67.0
Pt	PtS	PtS	19.9 ± 1	0.6	16.0	11.0
Au	Au^0	Au^0		—	1.4	0.1

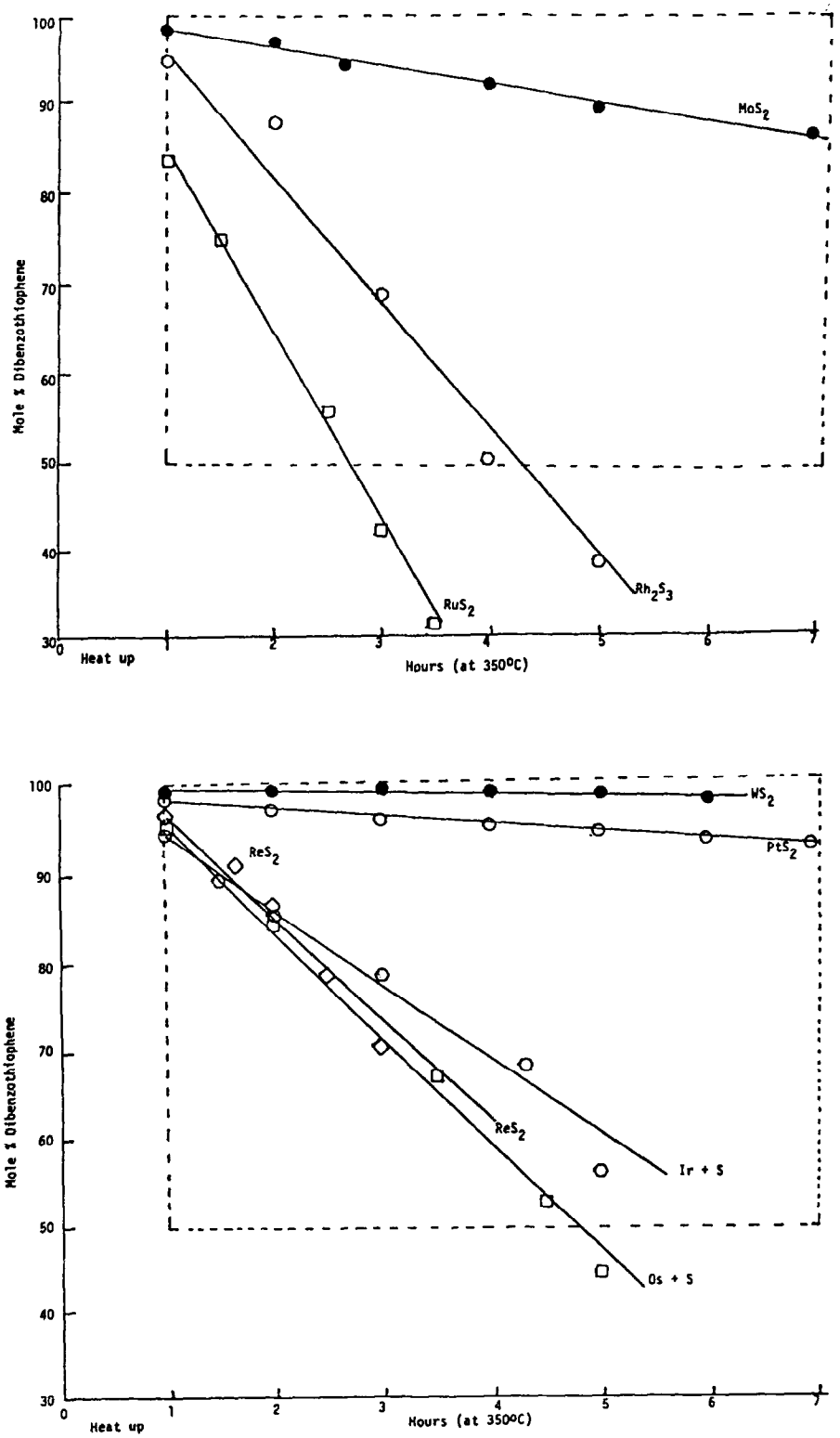

FIG. 3. Kinetic data for second- and third-row transition metals at 350°C.

catalyst basis. The order observed is

Second Row $RuS_2 > Rh_2S_3$
$> PdS > MoS_2 > NbS_2 > ZnS$,
Third Row $Os^0 + S > Ir^0 + S$
$> ReS_2 > PtS > WS_2 > TaS_2$.

This variation of the HDS activity per gram with periodic position is best illustrated in Fig. 4 and per millimole of metal in Fig. 5. The first-row metal sulfides are much less active than their second- and third-row members. In this case two maxima in HDS activity are attained. Chromium or Cr_2S_3 in Group VI displays the highest activity per gram and represents the first maximum. The Group $VIII_2$ and $VIII_3$ sulfides, Co_9S_8 and Ni_3S_2 constitute the second maximum.

When normalized to surface area (Fig. 6) only slight changes occur in the curves. For example, the most active catalysts at the peak of the curves change position; Rh becomes slightly more active than Ru, Os becomes more active relative to Ir, etc. Also the trends in the first-row activities become smoother. Maximum HDS activity is still attained by the second and third-row Group $VIII_1$ and $VIII_2$ metals but the order within the groups is changed.

Second Row $Rh_2S_3 \simeq RuS_2 > PdS > MoS_2$,
Third Row $Os + S > Ir^0 + S$
$> ReS_2 > PtS$.

In the case of the first-row metal sulfides, surface area normalization results in maximum HDS activity occurring for Groups VII and VIII sulfides, MnS and Ni_3S_2, respectively. These changes are not considered significant because the hydrodesulfurization activities of the sulfides *do not*, in general, correlate to BET surface areas due to specific morphological effects of structural and geometric origin. Thus, at this writing the normalization of the activity to a per metal basis or per gram basis best reflects the intrinsic activity of the transition metal sulfides. The nature of the transition metal in the sulfide (primary effect) dominates the role of anisotropy.

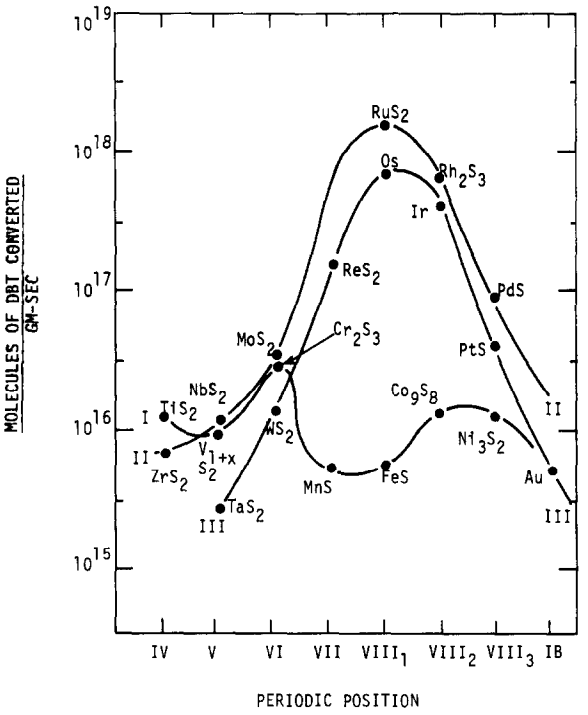

FIG. 4. Periodic trends for HDS of DBT/gram of catalyst at 400°C.

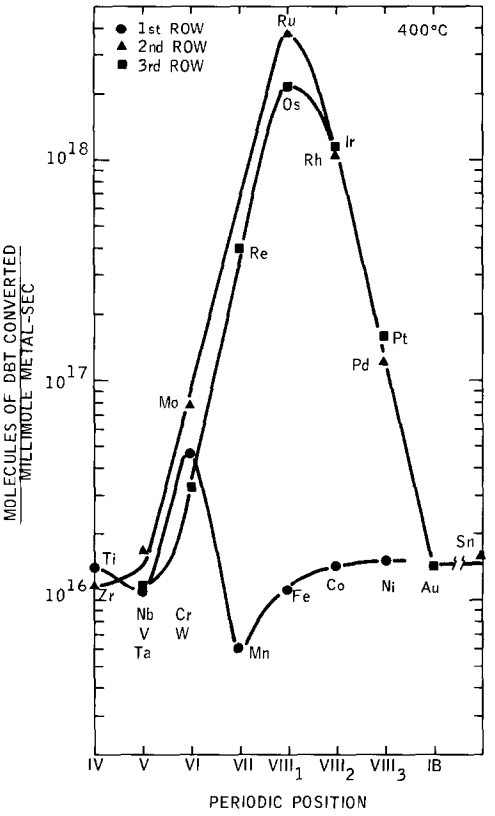

FIG. 5. Periodic trends for HDS of DBT/millimole of catalyst at 400°C.

Another set of HDS data obtained at a lower temperature, 350°C, and smaller particle size, 0.841/0.42 mm eliminates the mass transfer effects present at the higher temperature. Under these conditions, a variety of products are obtained: biphenyl, cyclohexylbenzene, and bicyclohexyl. Zero-order rate constants are calculated; see Figs. 7 and 8 and Table 4.

Maximum is obtained with RuS_2 in the second row and with ReS_2 in the third row:

Second Row $RuS_2 > Rh_2S_3 > MoS_2$,

Third Row $ReS_2 > Os + S > Ir^0 + S > PtS > WS_2$.

The variation of the HDS activity with periodic position is shown in Fig. 8 normalized to millimole of metal. As in the activity evaluation at 400°C, maximum activity is obtained with the second- and third-row Group $VIII_{1-3}$ sulfides. The only exception is the activity improvement displayed by ReS_2 when prepared from the tetrachloride instead of the pentachloride. The trends at 350°C are identical to those at 400°C. This effect of starting halide and preparative technique in general is a subject for further research.

DISCUSSION

The catalysis literature contains numerous examples of model reactions which display periodic maxima or "volcano" relationships. Sinfelt has reviewed broad relationships between catalytic activity of various metals in hydrogenation, hydrogenolysis, isomerization, hydrocarbon oxidation, and ammonia synthesis–decomposition reaction and their positions in the period table (*11*). The Group VIII transition metals display the maximum activity when compared to Groups IV–VII and

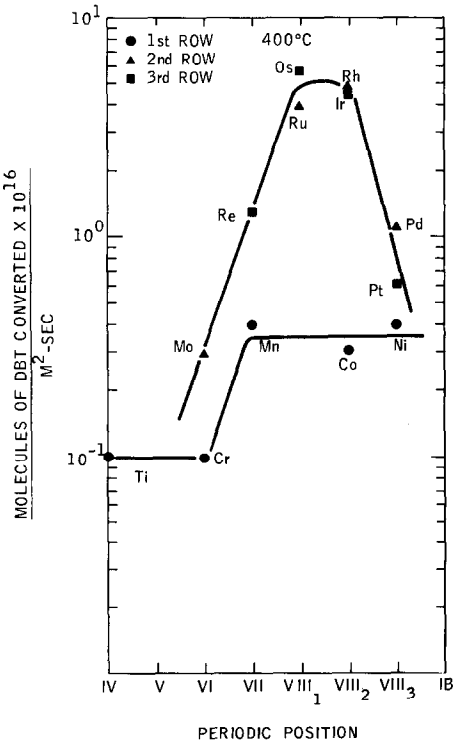

FIG. 6. Periodic trends for HDS of DBT/m² of catalyst at 400°C.

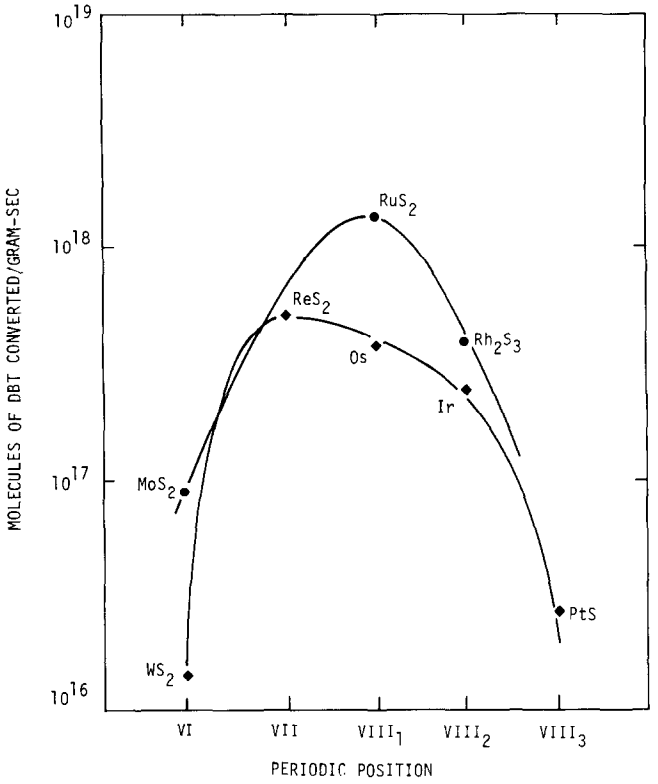

FIG. 7. Periodic trends for HDS of DBT/gram of catalyst at 350°C.

Groups I and IIB. Within Group VIII, the maxima fluctuate. In general the activity correlates with the electronic configuration of the *d* orbitals as "percentage *d* character" (of the metallic bond based on Paulings valence bond theory) or with the strength of the metal adsorbate bond.

In the case of transition metal sulfide catalysis, two studies are available which correlate activity with periodic position of the metal. Dowden (*12*) observed a twin-peaked pattern when catalytic activity for the reaction

$$CS_2 + 4\ H_2 \rightarrow CH_4 + 2\ H_2S$$

is plotted against the periodic position of the first-row transition metals. Maxima occur at Cr_2S_3 and between Co_4S_3 and NiS. The study was not extended to the second- and third-row sulfides. Wakabagashi *et al.* (*13*) recently discussed the HDS of thiophene over alumina-supported metals but found no smooth variaton of activity probably because of the superimposed effect of the Al_2O_3 support. They did, however, report high activity in Group VIII, particularly for Pt and Pd. These authors assert that the outer-shell *d* electrons and the atomic radii of the metals are the relevant factors in HDS activity. In addition the first long period displays the twin-peak phenomenon previously described by Dowden.

Many authors (*14–16*) recognize a relation among catalytic activity, the heat of adsorption of a reacting molecule, and the heat of formation of the corresponding compound. This relation, which is the well-known priniciple of Sabatier (*17*), states that compounds exhibiting maximum activity for a given reaction will have intermediate heats of formation. For sulfides catalyzing the HDS reaction the compounds exhibiting maximum activity will have intermediate heats of formation presumably

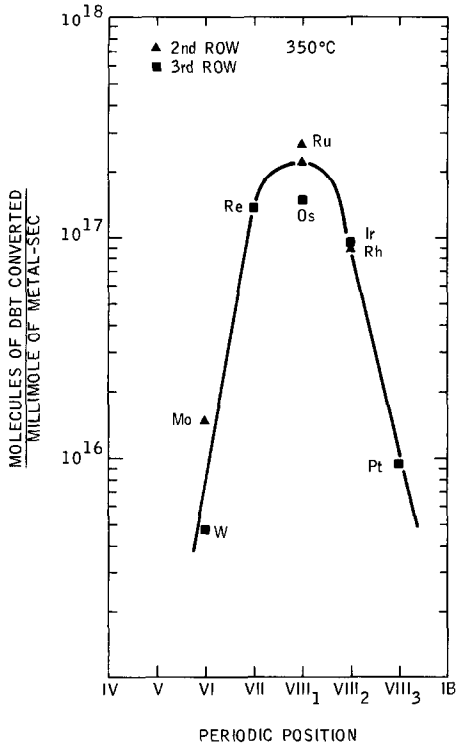

FIG. 8. Periodic trends for HDS of DBT/millimole of catalyst at 350°C.

because the stability of the surface complex formed by the sulfur-bearing molecule will be intermediate. Figure 9 illustrates that the heats of formation and, thus the metal sulfur bond strengths of the transition metal sulfides decrease continuously across the periodic table. For the second and third transition series the most active catalysts have intermediate values of the heat of formation (30–55 kcal/mole); see Fig. 10. This suggests that the strength of the metal–sulfur bond at the surface of the catalyst must not be too strong or too weak to obtain the maximum desulfurization rate. This seems to be consistent with the commonly accepted idea that sulfur vacancies on the surface of the catalyst are the active HDS sites (*1*). But this cannot be the entire picture since MnS in the first transition series falls within the required range for (51 kcal/mole) but shows very low activity.

Figure 11 shows Pauling percentage *d* character for the transition *metals* plotted against HDS activity at 400°C. The correlation which holds for the second and third, as well as the first row, is very good. This is true in spite of the fact that we do not know why this should be so. Perhaps percentage *d* character is just another reflection of the periodicity of the transition metal sulfides. Nevertheless, it remains a challenge to those interested in the fundamentals of catalysis to explain the origin of such correlations, which appear so frequently in catalysis.

From a solid-state chemistry point of view, the second- and third-row Group IV–VII sulfides are similar, very stable, layered structures with the metal occupying an octahedral (Ti, Zr, Hf, Te, Re) or trigonal prisomatic (Nb, Ta, Mi, W) coordination site. Elemental analyses indicate minimal sulfur deficiency in the activity-

TABLE 4

HDS Activity (at 350°C) of Bulk Sulfides[a]

Group	Metal	Molecules of DBT converted/mmole metal-sec × 10^{16} (350°C)	Molecules of DBT converted/g-sec × 10^{16} (350°C)
IV	Ti	—	—
V	V	—	—
VI	Cr	—	—
VII	Mn	—	—
$VIII_1$	Fe	—	—
$VIII_2$	Co	1.2	1.4
$VIII_3$	Ni	1.1	1.0
IV	Zr	—	—
V	Nb	—	—
VI	Mo	15.2	10
VII	Tc	—	—
$VIII_1$	Ru	251[b]	155[b]
$VIII_2$	Rh	90	59
$VIII_3$	Pd	—	—
IV	Hf	—	—
V	Ta	—	—
VI	W	4.8	1.5
VII	Re	137.3, 25.5[c]	70, 13[c]
$VIII_1$	Os	146.2	57
$VIII_2$	In	97.4	38
$VIII_3$	Pt	9.5	4.2

[a] Rate constants were calculated in a manner similar to that for the constants in Table 3.

[b] The value represented the average of several runs.

[c] The latter rhenium sulfide, $r_0 = 13$, was prepared from $ReCl_5$, while the former, $r_0 = 70$, was prepared from $ReCl_4$.

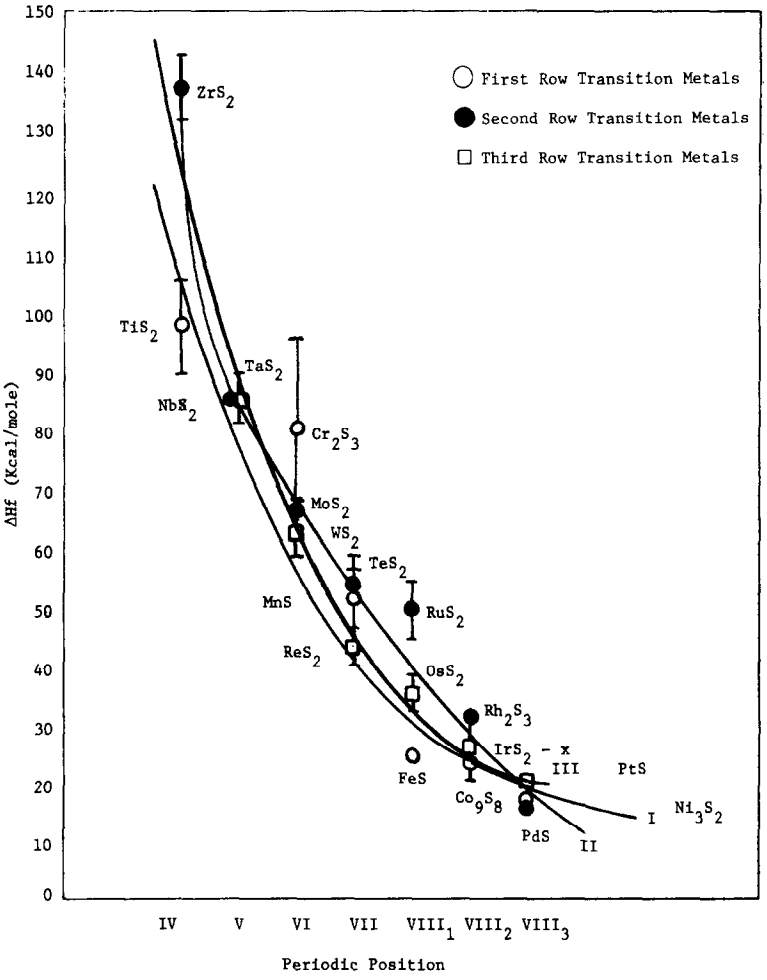

FIG. 9. Heat of formation of the transition metal sulfides as a function of periodic position (*10*).

evaluated materials. Once the Group $VIII_{1-3}$ metals are considered, the sulfide chemistry becomes very complex and each metal–sulfur system has its own unique chemistry. The structures and S/M ratios vary enormously.

The use of the non-aqueous precipitation standardizes the catalyst preparation. In addition, several novel amorphous and poorly crystalline layered structures are identified: poorly crystalline MoS_2 is located in a "rag structure" (*5*); OsS_2 is prepared in a layered structure as opposed to a pyrite structure. Finally, because this preparation results in solids which contain a substantial portion of amorphous material, the surface area predicted via X-ray line-broadening techniques and the BET surface area do not agree for several materials, e.g., MoS_2, ReS_2. Thus in these cases the activity does not correlate as well with BET surface area as it does with a chemisorphic technique, such as dynamic O_2 chemisorption (*6*).

CONCLUSION

The primary effect in the hydrodesulfurization of DBT by transition metal sulfides

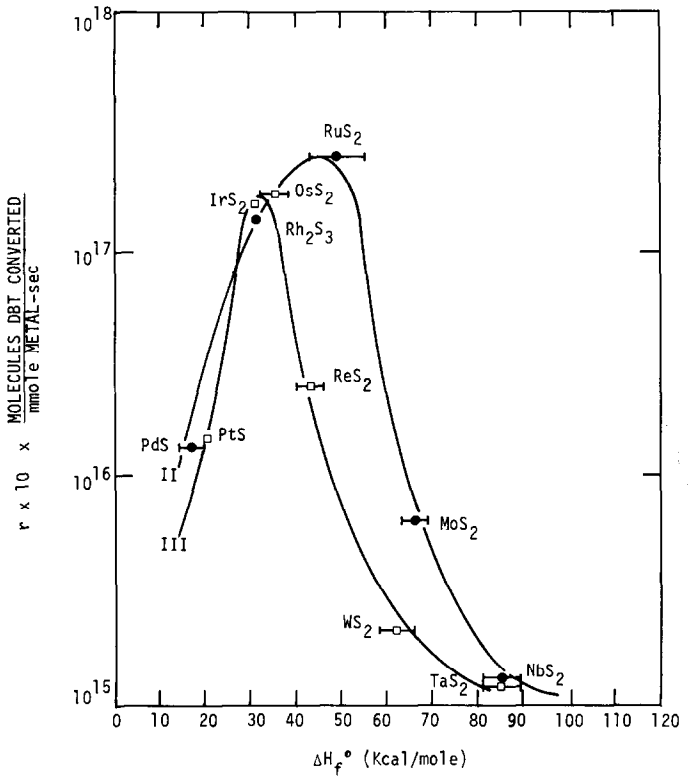

FIG. 10. HDS activity/millimole of catalyst as a function of heat of formation of bulk sulfide.

is "electronic" as it is in many other transition-metal-catalyzed reactions. The stable states of the catalysts under these conditions are either the bulk transition metal sulfides, or the surface sulfides as in the case of Os and Ir. The ability of the transition metal sulfides to catalyze this reaction varies over three orders of magnitude across the periodic table. The first-row transition metal sulfides are relatively inactive, but the second- and third-row transition metals show maximum activity near Ru and Os, yielding a typical "volcano" plot. The most active sulfide catalysts are those containing metals with maximum *d* character as shown in Fig. 11 as has been noted in other transition-metal-catalyzed reactions. In agreement with other transition-metal-catalyzed reactions, the heats of formation for maximum activity must take on inermediate values. The most effective catalysts appear to be those which have the ability to form and regenerate sulfur vacancies most easily within the catalytic environment.

The activity does not, in general, relate to BET surface area measurements, causing an uncertainty in the precise shape of the activity curves. Future work will concentrate on this secondary effect in hydrodesulfurization catalysis and turnover numbers are necessary in order to define the precise shape of the periodic trend curves. Nevertheless, the periodic trends presented in this report form the basis for understanding transition metal sulfide catalysts and for optimizing their properties for the stringent demands of future hydroprocessing applications.

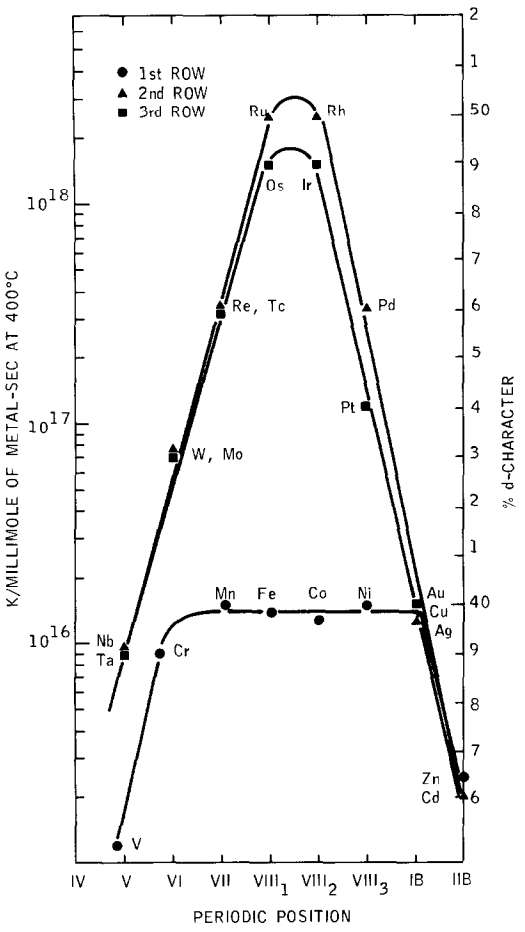

FIG. 11. Periodic trends versus Pauling % *d* character.

ACKNOWLEDGMENTS

The authors would like to thank F. R. Gamble and M. L. Gorbaty for useful conversations and B. A. Costellanto and F. J. Radloff for technical assistance.

REFERENCES

1. Weisser, O., and Landa, S., "Sulfide Catalysts: Their Properties and Applications," Pergamon, Oxford, 1973.
2. Donati, E. E., "Advances in Catalysis and Related Subjects," Vol. 8, p. 39. Academic Press, New York, 1956.
3. Voorhoeve, R. J. H., and Stuiver, J. C. M., *J. Catal.* **23**, 228 (1971).
4. Chianelli, R. R., and Dines, M. B., *Inorg. Chem.* **17**, 2758 (1978).
5. Chianelli, R. R., Prestridge, E. B., Pecoraro, T. A., and deNeufville, J. P., *Science* **203**(16), 1107 (1979).
6. Tauster, S. J., Pecoraro, T. A., and Chianelli, R. R., *J. Catal.* **63**, 515 (1980).
7. Passaretti, J. D., Collins, R. C., Wold, A., Pecoraro, T. A., and Chianelli, R. R., *Mat. Res. Bull.*, in press.
8. Whittingham, M. S., private communication.
9. Guinier, A., "X-Ray Diffraction." Freeman, London, 1963.
10. Mills, K. C., "Thermodynamic Data for Inorganic Sulfides, Selenides and Tellurides." Butterworths, London, 1974.
11. Sinfelt, J. H., *Progr. Solid State Chem.* **10**(2), 55 (1975).
12. Dowden, D., *Catal. Rev.* **5**(1), 1 (1972).
13. Wakabagashi, K., Abe, H., and Orito, Y., *Kogyo Kagaku Zasshi* **74**(7), 1317 (1971).
14. Sachtler, W. H. M. and Fahrenfort, J., *in* "Proceedings, 2nd International Congress on Catalysis, 1960," Vol. 1, p. 831.
15. Bond, G. C., "Catalysis by Metals." Academic Press, London/New York, 1962.
16. Tanaka, K., and Tamaru, K., *J. Catal.* **2**, 366 (1963).
17. Boudart, M., *Chem. Eng. Progr.* **57**(8), 33 (1961).